

Nanoscale

Accepted Manuscript



This is an *Accepted Manuscript*, which has been through the Royal Society of Chemistry peer review process and has been accepted for publication.

Accepted Manuscripts are published online shortly after acceptance, before technical editing, formatting and proof reading. Using this free service, authors can make their results available to the community, in citable form, before we publish the edited article. We will replace this *Accepted Manuscript* with the edited and formatted *Advance Article* as soon as it is available.

You can find more information about *Accepted Manuscripts* in the [Information for Authors](#).

Please note that technical editing may introduce minor changes to the text and/or graphics, which may alter content. The journal's standard [Terms & Conditions](#) and the [Ethical guidelines](#) still apply. In no event shall the Royal Society of Chemistry be held responsible for any errors or omissions in this *Accepted Manuscript* or any consequences arising from the use of any information it contains.

Effects of Morphology and Chemical Doping on Electrochemical Properties of Metal Hydroxides in Pseudocapacitors

Gyeonghee Lee,^a Chakrapani V. Varanasi,^{*,b} and Jie Liu^{*,a}

^a Department of Chemistry, Duke University, Durham, North Carolina 27708, United States.

Email: j.liu@duke.edu

^b Army Research Office, Durham, North Carolina 27703, United States.

Email: chakrapani.v.varanasi.civ@mail.mil

Keywords: energy storage, supercapacitors, nickel hydroxides, solvothermal, glucose additions

It is well known that both the structural morphology and chemical doping are important factors that affect the properties of metal hydroxide materials in electrochemical energy storage devices. In this work, an effective method to tailor the morphology and chemical doping of metal hydroxides is developed. It is shown that the morphology and the degree of crystallinity of Ni(OH)₂ can be changed by adding glucose to the ethanol-mediated solvothermal synthesis. Ni(OH)₂ produced in this manner exhibited increased specific capacitance, which is partially attributed to the increased surface area. Interestingly, the effect of morphology on cobalt doped-Ni(OH)₂ is found to be more effective at low cobalt contents than at high cobalt contents in terms of improving the electrochemical performance. This result reveals the existence of competitive effects between chemical doping and morphology change. These findings will provide important insights to design effective materials for energy storage devices.

Introduction

In the light of the gradual depletion of conventional energy resources and the resulting environmental crisis from heavy usage of fossil fuels, development of advanced energy storage devices including rechargeable batteries and supercapacitors is essential for the sustainable supply of energy to society needs.¹⁻⁴ Nickel hydroxides ($\text{Ni}(\text{OH})_2$), are widely used as electroactive materials in batteries and pseudocapacitors due to their cost effectiveness and well-defined redox processes.⁵⁻⁷ Hydrotalcite-like $\text{Ni}(\text{OH})_2$, particularly, have larger interlayer distance ($\sim 7 \text{ \AA}$) compared with that of their brucite-like counterpart ($\sim 4.6 \text{ \AA}$), showing interesting electrochemical activities.^{8,9} Their limited electrical conductivity ($10^{-5} \sim 10^{-9} \text{ S/cm}$), however, has been addressed as the most significant problem obstructing the ideal performance of $\text{Ni}(\text{OH})_2$ -based electrodes.^{9,10} Thus, developing effective strategies to assemble $\text{Ni}(\text{OH})_2$ -based electrodes with improved electrical conductivity is desired.

In recent years, extensive research has been carried out to improve the electrode conductivity through chemical doping and morphology control of active materials in nanoscale. Specifically, the electrode conductivity can be improved by chemical doping through which nickel (Ni) is partially substituted with other cations such as cobalt (Co), aluminum (Al), and zinc (Zn).¹¹⁻¹³ Doping Co particularly improves the electrochemical performance of $\text{Ni}(\text{OH})_2$ by increasing the electrical conductivity. For example, Co doped- $\text{Ni}(\text{OH})_2$ electrode exhibited high specific capacitance up to 1560 F/g, when the composition of the hydroxide is $\text{Co}_{0.5}\text{Ni}_{0.5}(\text{OH})_2$.¹⁴ This specific capacitance increase was attributed to the improved electrical conductivity when Co is doped in $\text{Ni}(\text{OH})_2$.^{14,15} On the other hand, reducing the size of active materials into nanoscale also enables reduction in resistance due to the decreased transport distance for both electronic and ionic species.^{16,17} As reported in

many articles, the size of Ni(OH)_2 materials can be tailored by adjusting the pH using chemical agents such as hexamethylenetetramine or alkali metal hydroxides and these size reduced- Ni(OH)_2 materials showed improved electrochemical characteristics owing to the facilitated mass transport.^{18,19} In our previous work, it was shown that the size of NiO platelets grown on carbon paper can be reduced and the specific capacitance of such NiO can be significantly improved by adding glucose to the ethanol-mediated solvothermal synthesis.²⁰ It is thus clear that both morphology control and chemical doping positively affect the electrochemical performance of Ni(OH)_2 when applied individually. However, it is unclear whether better electrochemical performances can be achieved when those two approaches are combined. Thus, this work is aimed at elucidating the mechanism and the combined effects of chemical doping and morphology control on the electrochemical properties of Ni(OH)_2 materials.

Here we show that the structural features compete with chemical doping in influencing the electrochemical performance of metal hydroxide electrodes. The morphology and the degree of crystallinity of Ni(OH)_2 were changed by adding glucose to the ethanol-mediated solvothermal synthesis. Ni(OH)_2 produced in this manner exhibited increased specific capacitance due to the reduced particle/flake size as a function of glucose concentration. In addition, Ni(OH)_2 prepared with glucose showed high water contents both on the surface and in the interlayer galleries. During the alcohol-based solvothermal treatment, glucose undergoes ethanolysis through which α -hydroxyl groups are substituted by ethoxy groups. They, especially at high glucose concentrations, limit the diffusion of Ni precursors during synthesis and therefore, inhibit the growth of Ni(OH)_2 particles into larger crystals. The effect of morphology control over a wide range of Co doped- Ni(OH)_2 ($\text{Co}_x\text{Ni}_{1-x}(\text{OH})_2$, $x = 0 - 1$) was investigated. Interestingly, the specific capacitance improvement introduced by glucose

was found to depend upon Co doping levels. It was more effective at low Co contents as compared to high Co contents. This tendency revealed the existence of competitive effects between chemical doping and morphology control. The possible reason for the competitive effect is the degree of inter-particle continuity and charge hopping. Specifically, more metal cation vacancies can exist on the surface of the highly amorphous materials, increasing the discontinuity between particles. Hence, in highly defective materials, the improvement due to charge hopping caused by chemical doping might become less effective. These findings will be important for designing effective materials for energy storage devices.

Experimental

Synthesis of $\text{Co}_x\text{Ni}_{1-x}(\text{OH})_2$. Metal hydroxides were synthesized via a solvothermal process. Typically, for $\text{Co}_{0.5}\text{Ni}_{0.5}(\text{OH})_2$ synthesis, 100 mg of $\text{Ni}(\text{NO}_3)_2 \cdot 6\text{H}_2\text{O}$, 100 mg of $\text{Co}(\text{NO}_3)_2 \cdot 6\text{H}_2\text{O}$, and 25 mg of urea were dissolved into 10 mL of ethanol. The precursor solution was transferred to a Teflon-lined autoclave vessel with a capacity of 20 mL. Then, the reaction mixture underwent a solvothermal reaction in the sealed container at 160 °C for 15 hours. The product was cooled to room temperature and then collected by vacuum filtration. The modified $\text{Co}_x\text{Ni}_{1-x}(\text{OH})_2$ by glucose was synthesized by adding D-glucose to replace portions of urea to the solvothermal process under the same conditions. Portions of the urea was replaced by glucose from 0% to 50% while the total amount of hydrolysis agent was fixed. Corresponding $\text{Co}_x\text{Ni}_{1-x}(\text{OH})_2$ synthesized in this manner was denoted as $\text{Co}_x\text{Ni}_{1-x}(\text{OH})_2$ -0%, $\text{Co}_x\text{Ni}_{1-x}(\text{OH})_2$ -10%, $\text{Co}_x\text{Ni}_{1-x}(\text{OH})_2$ -20%, and $\text{Co}_x\text{Ni}_{1-x}(\text{OH})_2$ -50%, respectively.

Characterization. X-ray diffraction (XRD) patterns were recorded with a Panalytical X'pert PRO MRD HR X-Ray Diffraction System equipped with Cu-K α radiation ($\lambda = 1.5405 \text{ \AA}$).

Scanning electron microscopy (SEM) was performed using a FEI XL30 SEM-FEG operating at 12 kV. The thermal analysis of samples was done by using a thermogravimetry (SDT 2960 Simultaneous DTA - TGA) system in air atmosphere in the temperature range from 30 °C to 800 °C with a heating rate of 10 °C/min. Fourier transform infrared (FTIR) spectra, over a range of 550-4000 cm^{-1} , were measured with Thermo Scientific Nicolet 380 FTIR spectrophotometer. The specific surface area of all $\text{Ni}(\text{OH})_2$ samples with the different glucose amounts were determined by nitrogen adsorption at 77 K. N_2 adsorption isotherms of samples were shown in **Figure S4**.

Electrochemical Measurements. Electrochemical measurements were carried out using a three electrode configuration: $\text{Co}_x\text{Ni}_{1-x}(\text{OH})_2$ electrode as a working electrode, a saturated calomel electrode (SCE) as a reference electrode, and a piece of Pt foil as a counter electrode. 2M KOH was used as an electrolyte. Working electrodes were prepared as following. The active material (~2 mg) was mixed with conductive graphite and polyvinylidene difluoride (PVDF) with the mass ratio of 70 : 20 : 10. The mixture was cast onto a piece of nickel foam and then dried in an oven (~70 °C) for 20 hours before using it as a working electrode. All electrochemical measurements were conducted using Bio-logic SP300 instrument. Cyclic voltammetry was performed in a potential window from -0.1 to 0.4 V at a scan rate of 5 mV/s. Chronopotentiometry was also performed in the potential range from -0.1 to 0.4 V at a current density of 1 A/g. Electrochemical impedance spectroscopy (EIS) measurements were conducted at a frequency range of 100 kHz ~ 0.1 Hz with AC voltage amplitude of 5 mV. The specific capacitance was calculated using the equation of $C_s = I / (dV/dt)m$, where I is the applied current, dV/dt is the potential change rate determined from galvanostatic charge-discharge curves, m is the mass of metal hydroxides.

Results and Discussion

Characterization of Ni(OH)₂ Synthesized with Glucose

Ni(OH)₂ samples were synthesized via ethanol-mediated solvothermal routes with various amounts of glucose in the reaction media. X-ray diffraction (XRD) patterns of resulting Ni(OH)₂ showed a systematic and unambiguous change in degree of crystallinity from highly crystalline phase to amorphous with increasing glucose concentrations (**Figure 1**). The observed peaks are assigned to (*hkl*) reflections of hydrotalcite-like Ni(OH)₂ (JCPDS No:38-0715). The intensity of all peaks, especially for (003) reflection, systematically decreased with increasing glucose concentrations. This systematic decrease in XRD peak intensity indicated the increasing disorder of the hydrotalcite-like features of Ni(OH)₂ as well as the decreasing size of crystallites. Additionally, the (003) reflection shifted to lower crystallographic angle as the glucose concentration increased. The corresponding interlayer distances were 7.01 Å, 7.15 Å, and 7.24 Å for Ni(OH)₂-0%, Ni(OH)₂-10%, and Ni(OH)₂-20%, respectively. This result revealed that Ni(OH)₂ synthesized with glucose can contain more interlayer water than that synthesized without glucose. Such interlayer water variations were detected in thermogravimetric analyses (TGA) as well as discussed later in detail.

The scanning electron microscope (SEM) images also showed the systematic morphology change of Ni(OH)₂ with increasing glucose concentrations (**Figure 2**). The size of Ni(OH)₂ flakes was significantly reduced with only 10% glucose. However, the density of flakes in this Ni(OH)₂ flower-shaped particle is considerably higher than that of Ni(OH)₂-0%. This tendency is consistent with our previous observation.²⁰ The size of flower-shaped particles started to be decreased as well as the flake size reduced when 20% glucose was added during synthesis. Finally, the size of Ni(OH)₂ flower-shaped particles synthesized with 50% glucose

was almost half of that of Ni(OH)₂-0%. Such systematic decrease in size of Ni(OH)₂ flakes/particles agrees well with the observed changes in XRD patterns, suggesting that the glucose addition to the alcohol-mediated metal hydroxide synthesis is an effective way to control the morphology as well as the degree of crystallinity.

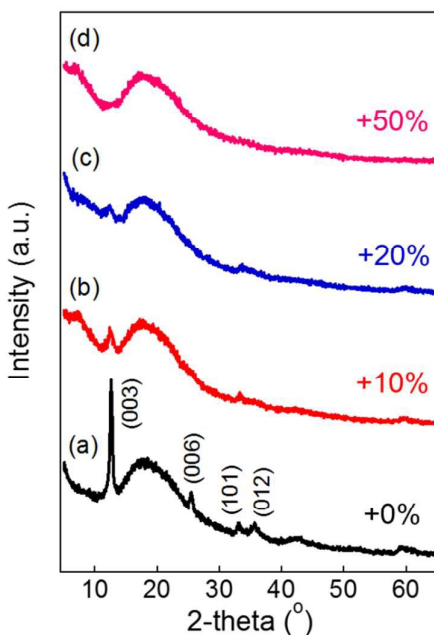


Figure 1. XRD patterns of Ni(OH)₂ synthesized with (a) 0%, (b) 10%, (c) 20%, and (d) 50% glucose.

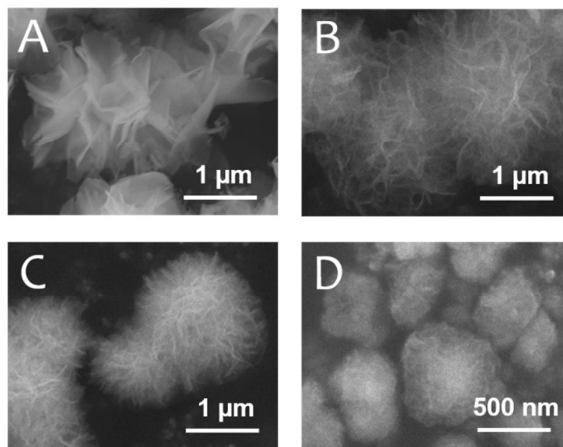


Figure 2. SEM images of Ni(OH)₂ synthesized with (A) 0%, (B) 10%, (C) 20%, and (D) 50% glucose.

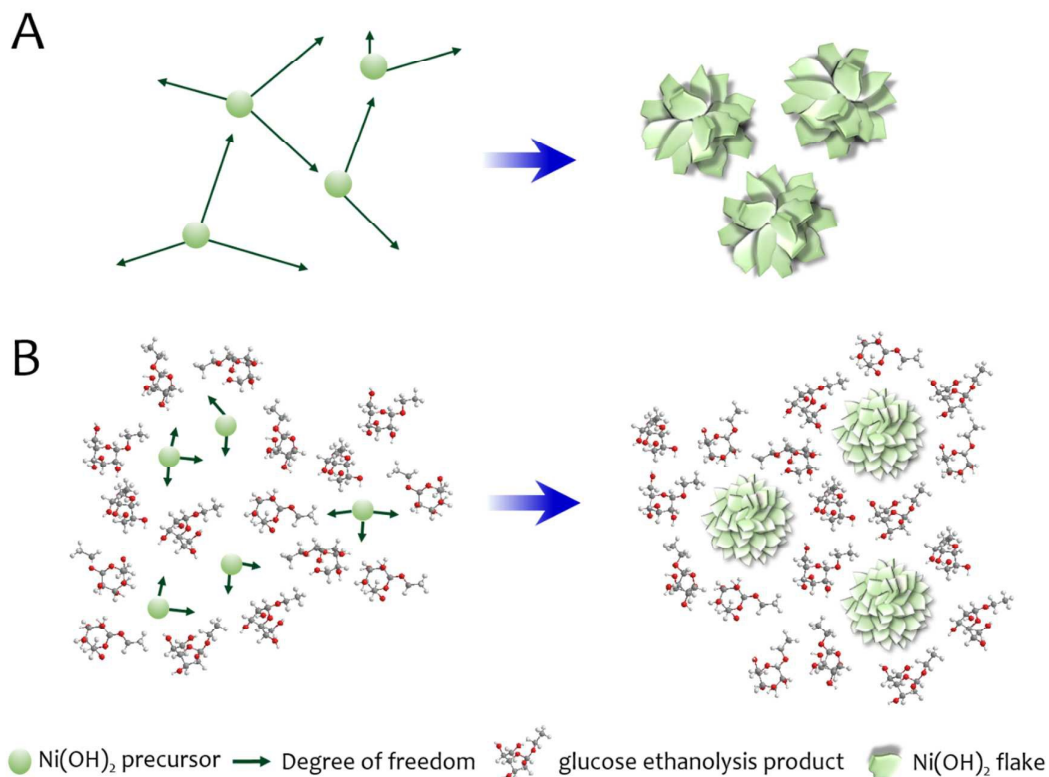
Figure S1A shows TGA results in the temperature range of 30-800 °C. As is shown, two distinct weight loss steps were observed in all the samples. The weight loss below 200 °C is ascribed to the removal of physically adsorbed water on the surface. It is possible to expect ethanol intercalation in Ni(OH)₂ interlayers during processing. However, fourier transform infrared (FTIR) analysis also indicated the absence of ethanol or glucose molecules in Ni(OH)₂ samples (**Figure S1B**). Ni(OH)₂ modified by glucose showed much higher surface water adsorption than that of Ni(OH)₂-0%. The weight loss in this region increased from ~5% to ~15% as the glucose concentration increased from 0% to 50%. This higher water adsorption is likely due to the increased specific surface area with the reduced size of flakes. Thus, the more surface becomes available for water adsorption. The sharp weight loss above 230 °C is associated with the elimination of hydroxyl groups in the layers and the evaporation of interlayer water molecules together with the simultaneous conversion into NiO (**Figure S1C**). Notably, the conversion into NiO started at lower temperature in samples with glucose. For example, the conversion starting temperature for Ni(OH)₂-50% was ~262 °C, which is about 20 °C lower than that of Ni(OH)₂-0% (~282 °C). This result indicated that the bond strength becomes weaker with higher glucose concentrations considering that the starting temperature for conversion into NiO can be affected by the bond strength between Ni and hydroxyl ions.¹⁹ Furthermore, the major weight loss above 230 °C of Ni(OH)₂ modified by glucose is much greater than that of Ni(OH)₂-0%. This greater weight loss might be due to the additionally intercalated water molecules in the interlayer of Ni(OH)₂ prepared with glucose addition. These results are consistent with the slight shift and decreasing intensity of (003) reflection in XRD with glucose addition, supporting that glucose can tailor the

morphology and degree of crystallinity efficiently during synthesis.

Role of Glucose in the Solvothermal Synthesis of Ni(OH)₂

To elucidate the possible mechanism of the modified morphology and the degree of crystallinity of Ni(OH)₂ with various amounts of glucose, a solvothermal treatment was carried out on the glucose dissolved-ethanol solution without metal hydroxide precursor. As depicted in nuclear magnetic resonance (NMR) spectroscopy, peaks corresponding to ethyl substituted glucose were observed instead of those originated from D-glucose (data not shown). Mass spectroscopic analysis also indicated the presence of ethyl substituted glucose molecule ($m/z = 208$). Based on these data, we hypothesized that these ethyl glucoside molecules can hinder the precursor diffusion and thus, inhibit the metal hydroxide growth during synthesis. The proposed mechanism of the modification of the morphology and the flake size is shown in **Scheme 1**. During the solvothermal treatment, glucose undergoes ethanolysis through which α -hydroxyl groups are substituted by ethoxy groups as shown in **Figure S2**.^{21,22} These ethyl glucosides are not as reactive as glucose without catalysts such as noble metals as α -hydroxyl groups are protected by ethyl groups.²² Converting ethyl glucosides back to glucose cannot occur.²² These glucose ethanolysis products are dispersed in the precursor solution and could confine the space for the nucleation and the subsequent growth of metal hydroxides. They, especially at high concentrations of glucose, limit the diffusion of precursors during synthesis and therefore, inhibit growth of metal hydroxides into larger single crystals. It should be noted that the glucose ethanolysis products are soluble in ethanol and thus, removed when Ni(OH)₂ powder is collected by filtration. FTIR spectra showed the absence of C-H or C-C groups, suggesting that these glucose ethanolysis products

are not included in $\text{Ni}(\text{OH})_2$ samples (**Figure S1B**). Unlike in the hydrothermal treatment of glucose, amorphous carbon formation was not observed due to the removal of α -hydroxyl groups, which participate in the condensation reaction for the polymerization of glucose prior to the carbonization.²³⁻²⁵



Scheme 1. Schematic illustration of proposed mechanism for the morphology modification of $\text{Ni}(\text{OH})_2$ by glucose in the solvothermal medium. (A) $\text{Ni}(\text{OH})_2$ precursors have sufficient spaces to diffuse and grow into large single crystals during synthesis without glucose. To reduce the surface energy, $\text{Ni}(\text{OH})_2$ flakes aggregate forming the large-sized flower-like structure. (B) The ethanolsis products of glucose are suspended in the precursor solution. $\text{Ni}(\text{OH})_2$ precursors have limited spaces for diffusion by ethyl glucosides. As a result, the size of $\text{Ni}(\text{OH})_2$ flower-like structure is significantly reduced.

To verify the proposed mechanism, the modified synthesis method including two-step solvothermal processes was designed. The purpose of this control experiment is to confirm whether glucose ethanolysis products limit the diffusion of precursor. In the first step, glucose dissolved-ethanol underwent solvothermal reaction without Ni(OH)₂ precursor. The amount of glucose dissolved in ethanol was corresponding to that of Ni(OH)₂-20% for this control experiment. After the first solvothermal reaction, a clear liquid product was obtained. In the second step, Ni(OH)₂ precursor was added to the product solution from first step and underwent another solvothermal process. **Figure S3A** shows SEM image of the morphology of Ni(OH)₂-20% obtained through this two-step synthesis. The size and the thickness of flakes decreased as observed in Ni(OH)₂-20% synthesized via one-pot solvothermal method. XRD pattern also exhibited the decrease in degree of crystallinity of Ni(OH)₂-20% prepared by this modified synthesis method (**Figure S3B**), supporting the validity of our hypothesis that the ethanolysis products inhibit the growth of metal hydroxides into large crystalline particles.

Effect of Morphology on Electrochemical Properties of Ni(OH)₂

The effect of controlling particle size and morphology on electrochemical performance of different Ni(OH)₂ samples was investigated by performing cyclic voltammetry (CV), galvanostatic charge–discharge, and electrochemical impedance spectroscopy (EIS) measurements. **Figure S5A** shows CV curves of Ni(OH)₂ synthesized with various amounts of glucose. A pair of redox peaks were exhibited in all samples originated from the reaction of Ni(OH)₂ + OH⁻ ↔ NiOOH + H₂O + e⁻.⁷ The Ni(OH)₂ synthesized with glucose showed higher peak currents than those without, indicating that the electrochemical performance can

be improved by reducing the particle size of the active material. The particle size and morphology controlled by glucose affected the surface area of Ni(OH)₂ samples. The changes in specific surface area and corresponding specific capacitance as a function of glucose concentrations were summarized in **Figure 3A**. The measured specific surface area values were 68.4, 110.8, 113.9, and 119.5 m²/g for Ni(OH)₂-0%, Ni(OH)₂-10%, Ni(OH)₂-20%, and Ni(OH)₂-50%, respectively. The specific surface area increased by ~60% with 10% glucose and then changed only slightly at higher glucose concentrations, indicating 10% glucose is sufficient for making a significant change in the surface area. The calculated specific capacitances of Ni(OH)₂ modified with 0, 10, 20, and 50 % glucose using discharge curves at the current density of 1 A/g (**Figure S5B**) were 784, 1055, 972, and 864 F/g, respectively. Generally speaking, the charge-discharge processes of Ni(OH)₂ involve the intercalation of protons into its lattice.²⁶ The presence of interlayer water molecules assists the proton diffusion.²⁶ In this regard, TGA results, where water contents in Ni(OH)₂ increase with glucose addition, also confirmed the improvements in specific capacitance by adding glucose. The specific capacitance was maximized at the glucose concentration of 10%. The sudden increase in specific capacitance from 784 F/g to 1055 F/g is believed to be due to the dramatic decrease in Ni(OH)₂ flake size as well as the resulting increased specific surface area with 10% glucose. The specific capacitance, however, decreased with the glucose concentration beyond 10%, which cannot be explained by the specific surface area alone. EIS results, discussed in the next paragraph, could explain the origin of decreased specific capacitance when glucose concentration in the precursor solution is higher than 10% despite the increased specific surface area.

Figure 3B shows Nyquist plots of Ni(OH)₂ synthesized with various amounts of glucose. The Nyquist plot is represented by the equivalent circuit as shown in **Figure 3B**. In the high

frequency region, the intercept at the real part (Z') is a combination of ionic resistance of the electrolyte, intrinsic resistance of the substrate, and contact resistance at the interface between active materials and the substrate (R_1).²⁷ The diameter of the semicircle at high frequencies represents the charge transfer resistance caused by Faradaic processes and the double layer capacitance, Q_2 (R_2).^{27,28} The straight line with a slope of 45° in the plot corresponds to Warburg resistance (W_2), and C_3 represents the Faradaic pseudocapacitance.²⁸ The equivalent series resistance (ESR), which includes R_1 , R_2 , and other resistances,²⁹ was determined using Nyquist plots and galvanostatic charge-discharge curves of Ni(OH)_2 samples and summarized in **Table S1**. As shown, ESR values of Ni(OH)_2 -10% ($\sim 2.3 \Omega$), Ni(OH)_2 -20% ($\sim 2.7 \Omega$), and Ni(OH)_2 -50% ($\sim 3.1 \Omega$) were smaller compared with $\sim 3.7 \Omega$ of Ni(OH)_2 -0%. This result suggested that the contact resistance between Ni(OH)_2 samples and the current collector reduced. This reduced resistance can be due to the increased specific surface area of Ni(OH)_2 samples synthesized with glucose (**Figure 3A**). These samples, thus, can have more surface area for a better contact with the current collector, making continuous conducting pathways. The impedance spectra reflects the transport properties of the active material affected by microstructural features such as orientation of grains.³⁰ Polycrystalline solids, in general, contain misorientated grains, leading to the limited transports for Faradaic processes compared with the single crystal.³⁰ These properties are particularly important for layered structured materials since ionic and electronic species transport across layers.³⁰ The transport properties, thus, affect the charge transfer resistance appeared as semicircles in the high frequency region. As shown in **Figure 3B**, the size of semicircles vary with glucose concentrations. The largest semicircle (the largest charge transfer resistance) is present in Ni(OH)_2 synthesized without glucose due to the less available active surface area for charge transfer compared with Ni(OH)_2 synthesized with glucose. The size of semicircles increased

again as glucose concentrations increased from 10% to 50%. This is attributed to the fact that misorientation of crystals becomes dominant with increasing glucose concentrations during synthesis, disturbing charge transfer paths. This agrees well with the XRD pattern where the structure of Ni(OH)₂ is more disordered at high glucose concentrations (**Figure 1**).

The cycle stability of Ni(OH)₂ synthesized without glucose and Ni(OH)₂ synthesized with 10% glucose was evaluated (**Figure S5C**). The capacitance of Ni(OH)₂ samples drastically increased initially and then, decreased by ~55% after 1000 cycles. Both Ni(OH)₂ prepared without glucose and Ni(OH)₂ prepared with 10% glucose exhibited a similar trend in the cycle performance, suggesting that morphology change does not affect the cycle stability of the electrodes.

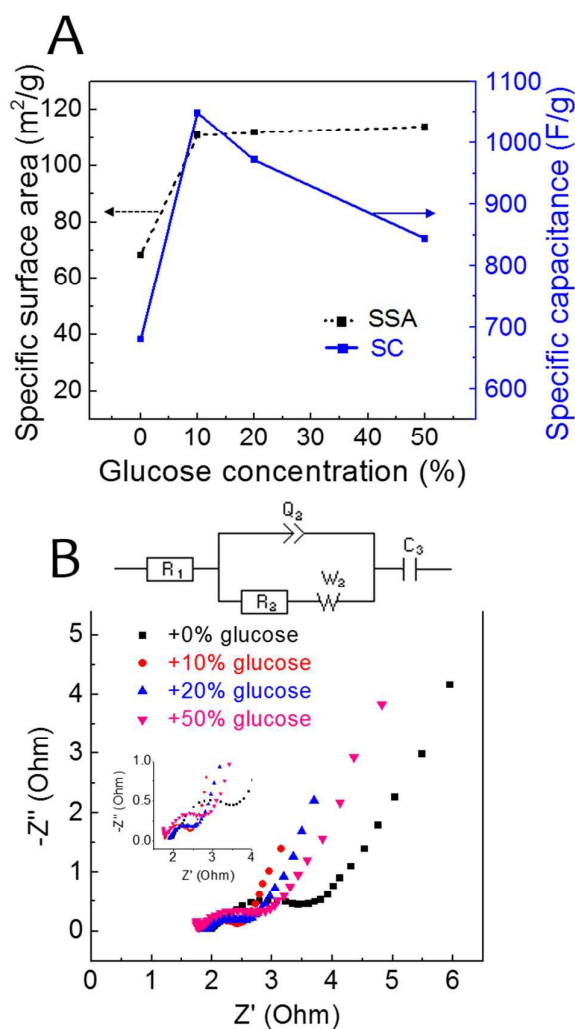


Figure 3. (A) Comparisons of the change in the specific surface area (SSA) and the specific capacitance (SC) of Ni(OH)₂ as a function of glucose concentration in the precursor solution. (B) Nyquist plots and a corresponding equivalent circuit of Ni(OH)₂ synthesized with and without glucose, showing that samples with glucose have a better contact with the current collector due to the reduced size of Ni(OH)₂ flakes.

Characterization of Co Doped-Ni(OH)₂ Synthesized with Glucose

To investigate the combined effect of morphology control and chemical doping on the specific capacitance, various amounts of Co doped-Ni(OH)₂ was synthesized with different concentration of glucose. The phase of the Co doped-Ni(OH)₂ was determined by XRD measurements. A typical XRD pattern of the Co_{0.5}Ni_{0.5}(OH)₂ is presented in **Figure S6**. Co_xNi_{1-x}(OH)₂ with other x values showed similar patterns. As is shown, the hydrotalcite-like feature was confirmed by the peak at 12.52° assigned to (003) reflection. The corresponding interlayer separation of 7.08 Å is larger than 7.01 Å of Ni(OH)₂ and smaller than 7.12 Å of Co(OH)₂ in this work, suggesting well-mixed Co and Ni in the layered hydroxide structure. With the addition of glucose, the intensity of XRD peaks gradually decreased. Such trends are similar to the observations as discussed earlier with pure Ni(OH)₂. **Figure S7** shows SEM images of Co_xNi_{1-x}(OH)₂ synthesized without glucose. The size of flakes slightly decreased as the concentration of doped Co increased. With the addition of glucose, the size of flakes were further reduced in all samples (**Figure S8**). These results are consistent with those of pure Ni(OH)₂, indicating that the glucose addition also can act as the effective morphology controlling agent for mixed metal hydroxide materials as well.

Electrochemical Performances of Co Doped-Ni(OH)₂

The electrochemical performance of Ni(OH)₂ with different amounts of Co (x = 0, 0.3, 0.5, 0.7, 1) was evaluated by CV and galvanostatic charge-discharge measurements. The representative cyclic voltammograms of Co_xNi_{1-x}(OH)₂ synthesized without glucose were shown in **Figure S9A**. A pair of redox peaks was explicitly observed in all Co_xNi_{1-x}(OH)₂, which corresponds to the combination of following Faradaic reactions of Ni(OH)₂ and Co(OH)₂: $\text{Co(OH)}_2 + \text{OH}^- \leftrightarrow \text{CoOOH} + \text{H}_2\text{O} + \text{e}^-$, $\text{CoOOH} + \text{OH}^- \leftrightarrow \text{CoO}_2 + \text{H}_2\text{O} + \text{e}^-$, and

$\text{Ni}(\text{OH})_2 + \text{OH}^- \leftrightarrow \text{NiOOH} + \text{H}_2\text{O} + \text{e}^-$.³¹ The absence of peak separation can be due to the well-mixed $\text{Co}(\text{OH})_2$ and $\text{Ni}(\text{OH})_2$ as revealed by the XRD result. Apparently, redox peaks are gradually shifted to a lower potential with the increase of Co content in $\text{Co}_x\text{Ni}_{1-x}(\text{OH})_2$. This result agrees with earlier reports, suggesting that the electrochemical behavior of metal hydroxides can be tuned by controlling their compositions.^{11,32,33} The same trend was also observed in CV curves of $\text{Co}_x\text{Ni}_{1-x}(\text{OH})_2$ synthesized without glucose.

The galvanostatic charge–discharge measurement was performed at 1 A/g. As shown in **Figure S9B**, charge-discharge plateaus shifted with increasing Co contents. This result agrees well with the trend in CV curves. The specific capacitance of $\text{Co}_x\text{Ni}_{1-x}(\text{OH})_2$ was determined and summarized in **Figure 4C** as a function of concentrations of Co and glucose. The substitution of Ni with an appropriate amount of Co clearly increased the specific capacitance of the electrodes. EIS results support this specific capacitance improvement. As summarized in **Table S1** and **Figure S10**, Co doping reduced ESR and increased the conductivity of $\text{Ni}(\text{OH})_2$ samples. These increased conductivities enable more effective charge storage. The enhancement in specific capacitance with Co doping on $\text{Ni}(\text{OH})_2$ can also be explained by the charge hopping model where the preferable charge propagation is through the next-nearest neighbors at a distance of $\sqrt{3}a$.³⁴ As seen in CV curves (**Figure S9A**), Co^{2+} oxidized to Co^{3+} at the lower voltage compared with $\text{Ni}^{2+}/\text{Ni}^{3+}$ pair during charge. For Co doped $\text{Ni}(\text{OH})_2$, Co^{2+} sites are oxidized Co^{3+} first and then, the positive charge might jump to the next-nearest neighboring Ni^{2+} (or Co^{2+}), inducing the earlier oxidation of Ni^{2+} to Ni^{3+} , and *vice versa* during discharge. As results, oxidation peaks shifted to lower voltage and reduction peaks shifted to higher voltage in case Co doped- $\text{Ni}(\text{OH})_2$. This charge hopping effect could be maximized when $x = 0.5$ in $\text{Co}_x\text{Ni}_{1-x}(\text{OH})_2$. Thus, the $\text{Co}_{0.5}\text{Ni}_{0.5}(\text{OH})_2$ showed the highest specific capacitance when synthesized without glucose.

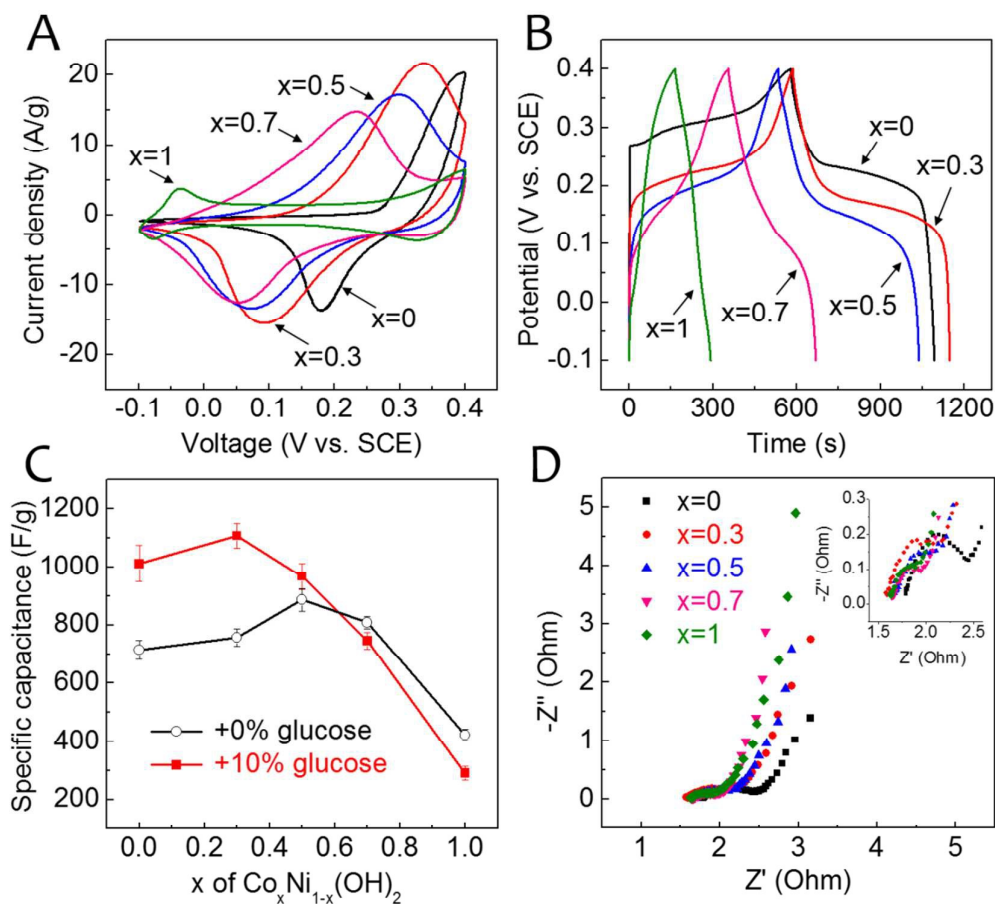


Figure 4. (A) Comparisons of CV curves of $\text{Co}_x\text{Ni}_{1-x}(\text{OH})_2$ synthesized with 10% glucose at a scan rate of 5 mV/s ($x = 0$ to 1), (B) galvanostatic charge-discharge curves of $\text{Co}_x\text{Ni}_{1-x}(\text{OH})_2$ synthesized with 10% glucose at a current density of 1 A/g, (C) trends in changes of the specific capacitance of $\text{Co}_x\text{Ni}_{1-x}(\text{OH})_2$ as functions of x . Each data point represents the average value of specific capacitance and error bars represent the standard deviation. (D) Nyquist plots of $\text{Co}_x\text{Ni}_{1-x}(\text{OH})_2$ synthesized with 10% glucose.

Effect of Morphology on Electrochemical Performances of Co doped-Ni(OH)₂

The electrochemical properties of $\text{Co}_x\text{Ni}_{1-x}(\text{OH})_2$ synthesized with glucose were also

investigated. The representative CV curves and galvanostatic charge-discharge curves were shown in **Figure 4A-B**. Corresponding shifts of redox peaks in CV and charge-discharge plateaus with Co doping were similar to those of $\text{Co}_x\text{Ni}_{1-x}(\text{OH})_2$ without glucose. Interestingly, improvements in specific capacitance of $\text{Co}_x\text{Ni}_{1-x}(\text{OH})_2$ synthesized with glucose varied according to the concentration of Co doped in the material. As summarized in **Figure 4C and Figure S11**, $\text{Co}_x\text{Ni}_{1-x}(\text{OH})_2$ prepared with glucose showed improved specific capacitance up to 50% of Co was doped in $\text{Ni}(\text{OH})_2$ samples. After 50% of Co doping, however, the specific capacitance improvement became less effective. This is likely due to the decreased crystalline size and the increased amorphousness of $\text{Co}_x\text{Ni}_{1-x}(\text{OH})_2$ caused by glucose. Such defective $\text{Co}_x\text{Ni}_{1-x}(\text{OH})_2$ samples contain more discontinuity between the particles compared with their bulk counterparts.^{35,36} In this case, the fastest charge propagation distance of $\sqrt{3}a$ is thought to become unavailable. Hence, the charge hopping might become less effective in such highly defective materials. EIS results also indicated that the improvement in electrochemical properties with morphology control is less effective when the active material is in the optimized composition (**Figure 4D and Table S1**). The smaller semicircles were present in $\text{Co}_x\text{Ni}_{1-x}(\text{OH})_2$ synthesized with glucose, showing reduced charge transfer resistance and increased specific capacitance. However, the decrease in ESR is smaller compared with $\text{Co}_x\text{Ni}_{1-x}(\text{OH})_2$ without glucose. Specifically, ESR value of pure $\text{Ni}(\text{OH})_2$ decreased by $\sim 1.4 \Omega$, whereas those of Co doped $\text{Ni}(\text{OH})_2$ decreased $\sim 0.5 \Omega$ when the size and morphology are controlled with 10% glucose. The addition of glucose, however, decreases the specific capacitance of $\text{Co}(\text{OH})_2$. This could be related to the mechanical instability of $\text{Co}(\text{OH})_2$ in basic electrolyte.³⁷ In addition, as discussed earlier, the particle/flake size of samples is significantly reduced. This size reduction could make more surface area of samples available for the contact with the electrolyte. In this regard, $\text{Co}(\text{OH})_2$ samples prepared with glucose

could be more easily dissolved into the corrosive KOH electrolyte before reaching the maximum capacitance after activation. Thus, the overall electrochemical performance of pure $\text{Co}(\text{OH})_2$ and $\text{Ni}(\text{OH})_2$ with high Co contents (e.g. $\text{Co}_{0.7}\text{Ni}_{0.3}(\text{OH})_2$) is less improved by morphology and size changes using glucose. These results imply that morphology control and chemical doping can competitively affect the overall electrochemical performances of metal hydroxide materials under certain conditions. Thus, finding the optimal dopants concentrations and controlling structural features that can complement the chemical doping are important to design effective electrode materials.

Conclusion

In conclusion, the addition of glucose to the ethanol-mediated solvothermal synthesis effectively reduces the particle size of metal hydroxide flakes. The specific capacitance is improved as a result of increased surface area and reduced particle size. Additionally, glucose modified-metal hydroxides under the optimized condition provide higher ion mobility due to the high interlayer water contents, which also can contribute to the improved specific capacitance. Ethyl glucosides are formed when glucose is added to the solvothermal synthesis of metal hydroxides. These ethyl glucoside molecules in the reaction mixture limit the diffusion of precursors during synthesis and therefore, inhibit the growth of $\text{Ni}(\text{OH})_2$ particles into larger crystals. Interestingly, specific capacitance improvements caused by glucose becomes less effective at high Co contents and more effective at low Co (high Ni) contents in Co doped- $\text{Ni}(\text{OH})_2$ materials, revealing the existence of competitive effects between the morphology and the chemical doping. These findings on combined and competitive effects of morphology and chemical doping will be important guideline for designing future materials

for high performance energy storage.

Acknowledgements

This work is supported by a research grant from Army Research Office (ARO) under contract W911NF-04-D-0001. However, any opinions, findings, conclusions or recommendations expressed in this material are those of the author(s) and do not necessarily reflect the views of the ARO. The authors also acknowledge the help of Minhee Lee in NMR analysis and the support from Duke SMIF (Shared Materials Instrumentation Facilities).

References

1. L. Dai, D. W. Chang, J. B. Baek and W. Lu, *Small*, 2012, **8**, 1130-1166.
2. P. G. Bruce, S. A. Freunberger, L. J. Hardwick and J. M. Tarascon, *Nature Materials*, 2012, **11**, 19-29.
3. A. S. Arico, P. Bruce, B. Scrosati, J. M. Tarascon and W. Van Schalkwijk, *Nature Materials*, 2005, **4**, 366-377.
4. Z. Yang, J. Zhang, M. C. Kintner-Meyer, X. Lu, D. Choi, J. P. Lemmon and J. Liu, *Chemical Reviews*, 2011, **111**, 3577-613.
5. J. Ji, L. L. Zhang, H. Ji, Y. Li, X. Zhao, X. Bai, X. Fan, F. Zhang and R. S. Ruoff, *ACS Nano*, 2013, **7**, 6237-6243.
6. H. Wang, H. S. Casalongue, Y. Liang and H. Dai, *Journal of the American Chemical Society*, 2010, **132**, 7472-7477.
7. J. W. Lee, T. Ahn, D. Soundararajan, J. M. Ko and J. D. Kim, *Chemical Communications*, 2011, **47**, 6305-6307.
8. P. V. Kamath and G. H. A. Therese, *Journal of Solid State Chemistry*, 1997, **128**, 38-41.
9. P. Olivia, J. Leonardi and J. F. Laurent, *Journal of Power Sources*, 1982, **8**, 229-255.
10. G. Wang, L. Zhang and J. Zhang, *Chemical Society Reviews*, 2012, **41**, 797-828.
11. Y. Cheng, H. Zhang, C. V. Varanasi and J. Liu, *Energy & Environmental Science*, 2013, **6**, 3314-3321.
12. Z. You, K. Shen, Z. Wu, X. Wang and X. Kong, *Applied Surface Science*, 2012, **258**, 8117-8123.
13. J. Huang, T. Lei, X. Wei, X. Liu, T. Liu, D. Cao, Y. Yin and G. Wang, *Journal of Power Sources*, 2013, **232**, 370-375.
14. X. Liu, R. Ma, Y. Bando and T. Sasaki, *Advanced Materials*, 2012, **24**, 2148-2153.
15. L. Xie, Z. Hu, C. Lv, G. Sun, J. Wang, Y. Li, H. He, J. Wang and K. Li, *Electrochimica Acta*, 2012, **78**, 205-211.
16. C. Liu, F. Li, L. P. Ma and H. M. Cheng, *Advanced Materials*, 2010, **22**, E28-E62.
17. D. R. Rolison, J. W. Long, J. C. Lytle, A. E. Fischer, C. P. Rhodes, T. M. McEvoy, M. E. Bourg and A. M. Lubers., *Chemical Society Reviews*, 2009, **38**, 226-252.
18. H. Jiang, T. Zhao, C. Li and J. Ma, *Journal of Materials Chemistry*, 2011, **21**, 3818-3823.
19. S. I. Kim, J. S. Lee, H. J. Ahn, H. K. Song and J. H. Jang, *ACS Applied Materials & Interfaces*, 2013, **5**, 1596-1603.
20. G. Lee, Y. Cheng, C. V. Varanasi and J. Liu, *The Journal of Physical Chemistry C*, 2014, **118**, 2281-2286.
21. L. Peng, L. Lin, J. Zhang, J. Shi and S. Liu, *Applied Catalysis A: General*, 2011, **397**, 259-265.
22. X. Hu, C. Lievens, A. Larcher and C. Z. Li, *Bioresource Technology*, 2011, **102**, 10104-10113.
23. K. Aydıncak, T. Yumak, A. Sınağ and B. Esen, *Industrial & Engineering Chemistry Research*, 2012, **51**, 9145-9152.
24. C. Falco, N. Baccile and M. M. Titirici, *Green Chemistry*, 2011, **13**, 3273-3281.
25. M. M. Titirici, R. J. White, C. Falco and M. Sevilla, *Energy & Environmental Science*, 2012, **5**, 6796-6822.
26. T. N. Ramesh, R. S. Jayashree and P. Vishnu Kamath, *Journal of The*

- Electrochemical Society*, 2003, **150**, A520-A524.
27. M. S. Wu, Y. A. Huang and C. H. Yang, *Journal of The Electrochemical Society*, 2008, **155**, A798-A805.
 28. H. Yan, J. Bai, J. Wang, X. Zhang, B. Wang, Q. Liu and L. Liu, *CrystEngComm*, 2013, **15**, 10007-10015.
 29. W. Chen, R. B. Rakhi, L. Hu, X. Xie, Y. Cui, and H. N. Alshareef, *Nano Letters*, 2011, **11**, 5165-5172.
 30. E. Barsoukov and J. R. Macdonald, Impedance Spectroscopy. *Wiley Interscience*, 2nd Edition, 2005.
 31. Y. Tao, L. Zaijun, L. Ruiyi, N. Qi, K. Hui, N. Yulian and L. Junkang, *Journal of Materials Chemistry*, 2012, **22**, 23587-23592.
 32. M. Vidotti, M. R. Silva, R. P. Salvador, S. I. C. de Torresi and L. H. Dall'Antonia, *Electrochimica Acta*, 2008, **53**, 4030-4034.
 33. X. Sun, G. Wang, H. Sun, F. Lu, M. Yu and J. Lian, *Journal of Power Sources*, 2013, **238**, 150-156.
 34. R. Ma, J. Liang, X. Liu and T. Sasaki, *Journal of the American Chemical Society*, 2012, **134**, 19915-19921.
 35. W. Sugimoto, H. Iwata, K. Yokoshima, Y. Murakami and Y. Takasu, *The Journal of Physical Chemistry B*, 2005, **109**, 7330-7338.
 36. V. Biju and M. A. Khadar, *Materials Research Bulletin*, 2001, **36**, 21-33.
 37. M. Suksomboon, P. Srimuk, A. Krittayavathananon, S. Luanwuthia and M. Sawangphruk, *RSC Advances*, 2014, **4**, 56876-56882.

The Table of Contents Entry

Structural features of cobalt doped-nickel hydroxide materials can be controlled via ethanol-mediated solvothermal synthesis with glucose additions. Such rationally designed metal hydroxide materials show improved electrochemical performances. This improvement, however, is observed only at low cobalt contents in the materials. These results suggest that finding optimal doping concentrations and morphology are key to design high performance electrode materials.

Keywords: energy storage, supercapacitors, nickel hydroxides, solvothermal, glucose additions

Gyeonghee Lee, Chakrapani V. Varanasi* and Jie Liu*

Effects of Morphology and Chemical Doping on Electrochemical Properties of Metal Hydroxides in Pseudocapacitors

